Improvement of photovoltaic conversion in sexithiophene-based photovoltaic cell with self-assembling dipole molecules

H. BEDIS OUERGHEMMI[*], F. KOUKI, H. BOUCHRIHA, F. GARNIER
UMAO, Faculté des Sciences de Tunis, Campus Universitaire, 2092 El-ManarI, Tunis, Tunisia

In this paper, we study in the first the electrical and optical behaviours of organic photovoltaic cell based on thin film of sexithiophene (6T). We describe from current vs. applied voltage and impedance spectroscopy the mechanisms controlling conduction in this device. From absorption spectra, the action spectra and their modulation by Gosh model; we can evaluate motilities of generated photocarriers. In the second, we study the effect self-assembled dipole molecules (SAM) of benzoic acid on the photovoltaic behavior. From current-voltage characteristics after illumination we can estimate photovoltaic parameters of elaborated samples that shift according to orientation and the magnitude of dipole moment of molecule SAM. This Improvement involves a remarkable increase of the efficiencies of these devices.

1. Introduction

Research on photovoltaic devices based on organic semiconductor materials know a great raise the last years [1,2,3]. That is justified by the low cost of these materials, their great diversity and the relative facility of manufacture of components with simple technologies. In addition to the choice of materials and their film structure, morphology, and thickness, the interface between the organic materials and the electrodes is critical to device performance. The development of organic photovoltaic cells (OPVCs) is still a matter of research despite the low efficiency relatively to mineral ones which is precisely a crucial factor for their commercialization. This is due to mainly two reasons: the first is the low dielectric constant of organic semiconductors (~3) relatively to that of inorganic ones (~10). This property makes photo-excited electron-hole geminate pairs (excitons) much more bound, due to columbic interaction, in organic materials. The second crucial factor is the low mobility of carriers in organic semiconductors [4]. Excitons in organic semiconductors are Frenkel-type with a binding energy in the order of some tenths eV [5]. This relatively high binding energy prevents these photo-excited species from dissociating which reveals low free carrier production efficiency. Organic systems are gradually finding their way to applications in electronics and optoelectronics, based in oligothiophenes α-nT and it have been used as active layers in organic photovoltaic cells (OPVCs) [1,6-8]. The performances of these components require in addition to control the synthesis and development of the thin layers, a better comprehension of the orientation and structural organization of these molecules during their deposit in thin films. A better understanding of the correlation between the optical and electrical properties is needed for the improvement of oligothiophene based devices. The principle of operation of the components is based on the conversion of a light signal into an electric signal: photocurrent. They exploit fundamental effects such as absorption of the light, the photogeneration of the charge carriers, photovoltaic conversion. In our study we interest in especially in sexithiophene du to their greater stability, chemical purity with weak gap (2.3 eV). The most probable sketch to account for photocurrent observed experimentally in OPVCs is that free carriers are produced from dissociation of exitons by interaction with the metal/Semiconductor interface [5]. Self Assembled Monolayers (SAMs) which were widely used in OLEDs, are supposed to induce modification of metallic electrode work function that improve of carrier injection into the organic semiconductor [9-12], is also used in OPVCs in order to control photocarrier generation and to provide an increase in device efficiency. The photogeneration of free carriers results from dissociation of Frenkel type excitons that lying in the built in potential.

In this paper, we investigate a qualitative study of electrical and optical characteristics of photovoltaic cell base on sexithiophene and sandwiched between indium tin oxide (ITO) and aluminium(Al), in witch we describe mechanisms controlling conduction, evaluate the parameters that switch the generated photocarriers. We compare afterwards the J-V characterization in illumination by two types of lamp tungsten and Xenon lamp. Furthermore, we examine the grafting effect of self-assembled monolayer of two types of dipolar molecules of benzoïc acids on ITO substrate used as anode of our

photovoltaic cell. We investigate the role of oriented dipole molecule into charge carrier photogeneration and the efficiencies of these devices.

2. Experimental

2.1 Preparation of ITO

The purpose of the preparation of the ITO is to eliminate the impurities and to increase its surface reactivity and the interactions with the grafted molecules. For the whole of our experimental work, the glassmaking and the whole of material are carefully past with the hydrogen flame in order to avoid to the maximum any contamination which may trouble grafting of SAM. Prior to SAMs grafting ITO substrates, provided by SOLEMS, were carefully cleaned according to the following protocol: first the samples are immerged in an ultrasound bath of ultrapure water for 30 mn, second we rinse these samples in NaOH pur (30%) during 15 mn and third, we emerge the sample in pure sulphuric acid (98%) during 1mn after that than we rinse the samples with ultra pure water during 1mn and finally drying the samples with argon. This chemical treatment is used in order to render surface more hydrophilic and reactive with respect to grafted SAM.

2.2 Preparation of SAM

SAMs were obtained by solution dipping of cleaned ITO substrates according to the following procedure: we prepared three solutions with the molecules (Fig.1). We use pure solution of 2ml of 4-Aminobenzoic acid (ABA), 4-Nitrobenzoic acid (NBA). Typical examples of such molecules used are given in Fig. 1a and 1b. All the experimental steps were performed at room temperature.
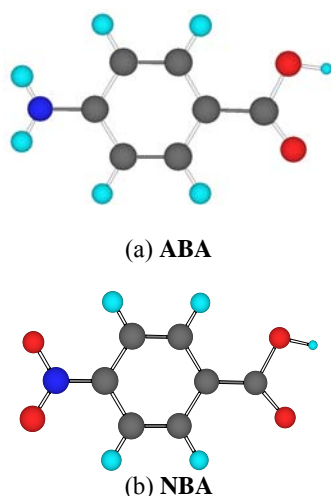

(a) **ABA**

(b) **NBA**

Fig.1. Chemical structure of (a) p-Aminobenzoic acid ABA and (b) p-Nitrobenzoic acid NBA

2.3 Devices making: photovoltaic cells

Sexithiophene (Fig. 2) was synthesized according to the description given in [13,14]. Studies of this molecule have showed [15] that all the six thiophene rings have practically identical geometry, except for the two external C=C double bonds which are shorter than all the others.
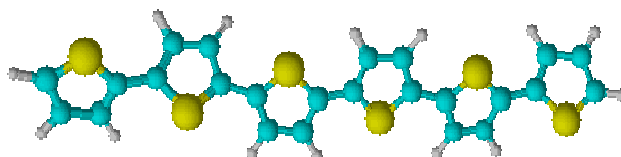

Fig. 2. Chemical structure of sexithiophene (α-6T).

In order to obtain comparable results either between both SAM coated ITO and between SAM-coated and pristine ITO we performed both sexithiophene and aluminum coatings in the same (coup). We deposited 80 nm of 6T by thermally evaporation process under vacuum simultaneously on three substrates: two of them were coated with SAMs one with NBA and the other with ABA, the last one were just cleaned substrates. The speed of deposition is 1Å/s with very slow sublimation to avoid degradation. Prior, a rapid deposition of a 30 nm of aluminum (Al) top contact through a shadow mask under 10^{-6} torr, leading to final sandwich structures ITO/SAM/6T/Al and ITO/6T/Al (Fig.3). Each sample consisted of two pixels each of which had a rectangular shape of surface 0.2 cm².
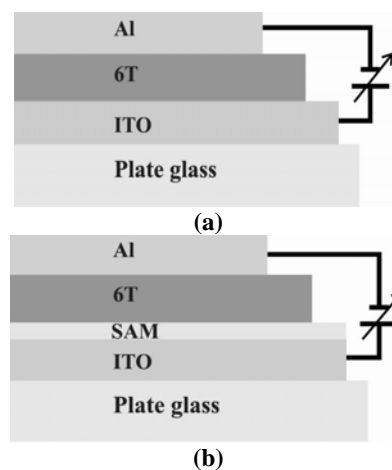

(a)

(b)

Fig. 3. Structure of photovoltaic cells: (a) without SAM, (b) with SAM .

2.4 Experimental devices of characterization

J-V characterizations of these cells obtained were carried out by Keithley 2400 electrometer. The measurements where performed in dark and under white light from a 100W tungsten lamp and from 100W XBO lamp.

Absorption spectra have been recorded with a Carry 500 UV-VIS-NIR spectrophotometer that directly gives

the variation of optical density D.O or absorbance vs. wave length of thin film of 6T. The photocurrent action spectra were measured by illuminating the cell through the al electrode with Xenon lamp (XBO, 150W), towards the monochromator (Acton Spectrapro150) of speed 1nm/s and by using a synchronous detection (ATNE ADS 2) to analyse the modulated signal. All measurements are taken in the ambient air and at room temperature on the optical bench by illumination of the cell through the semi-transparent Aluminium electrode and through ITO. The spectrum is corrected while placing a photodiode with silicon (UDT) in the place of the sample.

3. Results and discussion

3.1 Electrical characterization of ITO/6T/Al

3.1.1 Current-voltage characteristics in the dark

The current-voltage characteristic of our device without SAM with the active area of 0.2 cm² in linear and logarithmic current density log(J) vs. the applied voltage plot was shown in Fig. 4. J-V characteristics recorded at ambient temperature show a typical diode behavior with significant rectification ratio with onset voltage V_{th} is about 7 V. According to J-V curves of this device it was find that 6T behaves as p-type organic semiconductor, which forms a Schottky barrier at Al/6T interfaces in weak applied bias voltage. The plots of the logarithmic current density log(J) vs. log(V) in inside Fig.4, indicate that in the weak voltage region (<1 V), injection is limited by the electrode through thermoionic emission above Richardson-Schottky barrier. According to this model, we can estimate the potential barrier height ϕ_b as 0.39 eV. Above 1V the plot of log(J) vs. log(V) shows space charge limited current (SCLC) according to traps free Child's law and follows SCLC regime in a shallow voltage region comprised between 1 and 2.2 V.
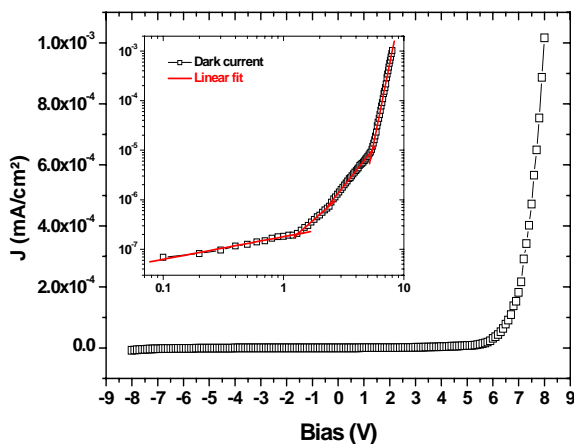
The estimate effective mobility in case is about $1.5 \, 10^{-6}$ cm²V⁻¹s⁻¹. Hence, the sample show two different TCLC mechanisms related to two different kinds of traps. The first, observed between 2.2 and 5 V is probably attributed to structural defects. The second, which occurs in region above 5V seems to be related to chemical defects, where the density is independent of structural order in the film 6T. The device follows in the regime, Traps Charge Limited Current (TCLC), afterwards the current rapidly increases, indicates traps-filled limit (TFL) conduction. The total trap density can estimate as $1.6 \, 10^{17}$ cm⁻³. 0.
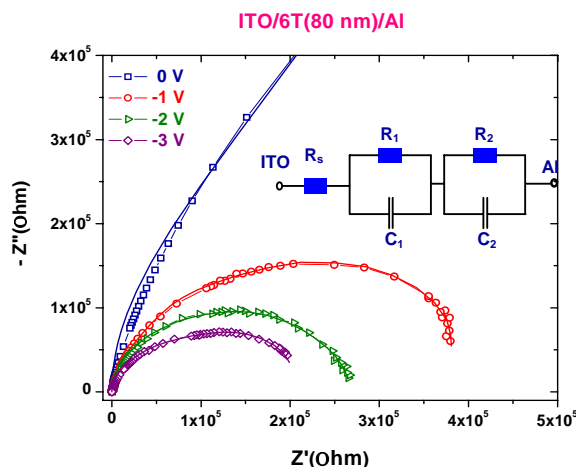
3.1.2 Impedance spectra of ITO/6T/Al

Fig. 5. Diagram Nyquist of ITO/6T/Al with digital simulation and their equivalent circuit

Fig. 5 shows the Cole–Cole plot (Z" vs. Z') in the complex impedance plane. We notice a reduction in the impedance with the applied voltage, moreover from tension equal to -1 V, we has a pace in half-circle, characteristic of a resistance in parallel with a capacity. Actually it will be seen that by increasing the scale with the low impedances, we observe two half-circle where the second has a larger ray. Modeling by the program OriginLab allow us to find the equivalent circuit of these curves. Indeed independently of applied voltage, we find an equivalent editing containing two circuit in series (R_p // C_p) with the contact resistance Rs (inside Fig.5). The first circuit is due to the space charge zone container a resistance R_1 parallel to the capacity C_1 , a second (R_2 // C_2) is due to the volume of the active layer (6T). We assemble the results of simulation in the Table 1.

Fig. 4. Characteristics I-V of ITO/6T/Al structure in the dark Inside log(J) vs. log(V) plot.

Table1 Simulation results of impedance spectrum.

Polarity (v)	Rs (Ω)	$R_1 \times 10^5$ (Ω)	C_1 (μF)	$R_2 \times 10^5$ (Ω)	C_2 (μF)
0	86.2 ± 0,2	20 ± 5	7,5 ± 0,5	4 ± 0,5	3,5 ± 0,1
-1	47,6 ± 0,1	1,3 ± 0,2	7,3 ± 0,2	2,8 ± 0,3	25 ± 5
-2	47,7 ± 0,1	1,1 ± 0,1	7,3 ± 0,6	1,5 ± 0,0	30 ± 0
-3	48,1 ± 0,2	0,8 ± 0,1	6,6 ± 0,6	1,1 ± 0,1	35 ± 5

The table1 assemble the results of simulation of the Nyquist, and show that R_S is practically independently of the tension applied and remains constant. This resistance corresponds to the contacts ITO/6T or Al/6T. Moreover, R_S is very weak as R_1 and R_2 for all the applied voltage that corresponds as ohmic contact resistance. This enables to envisage a majority current of holes and limited by the space charge. R_1 values are practically independent of the applied tension but R_2 decrease by increasing the biasing at the weak frequencies. The capacity C_1 remains constant under polarization, this invariance confirms a behavior of space charge limited current (SCLC). Capacity C_2 present dependence of applied voltage and to little reach a maximum value of 35μF, probably due to the existence of traps in volume which take part in the role of acceptors [16].

3.1.3 Current-voltage characteristics after illumination

Fig. 6 shows the tendency observed of ITO/6T/Al under illumination by a tungsten lamp and Xenon lamp in side the Al. This tendency suggested us using a more effective source of light i.e. emission spectrum covers better that with the absorption of our active layer (6T). Thus the maximum of absorption of the sexithiophene (~360nm) is located in UV and that in addition the tungsten lamp emits very little light in this spectral area. We thus used a Xenon lamp in order to maximize the absorption of photons and photogenerate excitons.
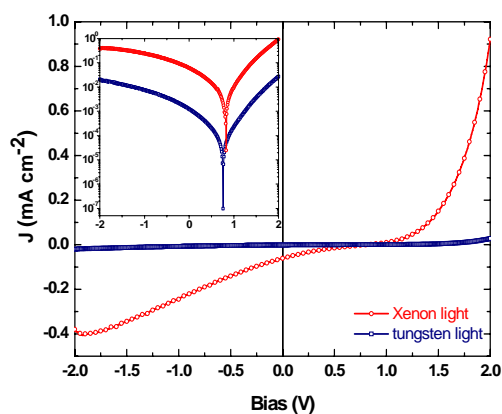
Table 2. Photovoltaic parameters of ITO/6T/Al cell after illumination by tungsten and Xenon lamp.

	V_{OC} (V)	Jsc (μA/cm²)	FF(%)	$(\eta \pm 0,1) \times 10^{-2}$ (%)
ITO/6T/Al (tungsten)	0,67	0,48	15,5	0,83
ITO/6T/Al (Xenon)	1,18	0,48	28,75	2,7

By observing Fig. 6 and photovoltaic parameters in Table 2, we remark clearly that the potential of open circuit and efficiency of (ITO/6T/Al) increased considerably compared to the illumination by a tungsten lamp. This increase is probably ascribable at the photogenerate carrier's rate of factors which are much more significant with xenon lamp. In the continuation we will study from J-V characteristic under Xenon illumination, the effect of dipolar SAM molecules with permanent dipole moment in photovoltaic conversion.

3.2 Optical characterization

We presented on the Fig. 7, the action and the absorption spectra relating to the structure ITO/6T/Al under illumination on side Al and ITO. We notice a weak absorption which starts in large wavelengths (weak energies) followed vibronic counterparts and at the end a strong absorption towards the lowest wavelengths. This absorption originate from the transition $\pi - \pi^*$ of insulated molecules that is allotted to the transitions S_0-S_1. From energy point of view, we remark that absorption in stronger wavelengths is non-existent. In addition, in this area the light crosses the sample without being absorbed, under this energy level the light does not induce any electronic transition and we are in height in the gap of 6T that is about 2.2 eV.
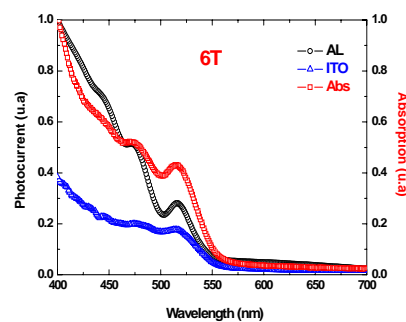

Fig. 6. Characteristics I-V of ITO/6T/Al structure under illumination with tungsten lamp and Xenon lamp. Inset semi-logarithmic plot.

Fig. 7 Action and absorption spectrum of the ITO/6T/Al structure.

The action spectrum of the photocurrent of a photovoltaic cell expresses the variation of the photocurrent according to the wavelength of light. According to result of Fig .7, it seems that the illumination on side Al create excitons close to the active region which is located at the Al/6T interface. This process generates a significant photocurrent due to the dissociation of strongly bounded excitons into free charge carriers or trapping off carriers trapped by these excitons [17]. The process of collection of the carriers is in agreement with strong absorption in this region. Electrically, we considering that the Al/6Tcontact corresponding to a weaker work function of metal (ϕ_{Al} = 4.2eV and ϕ_{ITO} = 4.8eV) which is active in the mechanism of creation of the carriers. Then, when illuminate on the side of Al, the pairs of carriers would be create in the active zone and their separation at interface give a photocurrent, but when we illuminate on the ITO side, the photocurrent spectrum is less intense and present different profiles according to the polarization of the incident light. In this case the diffusion length of exciton is short compared to the optical length of absorption and the excitons which are often photogenerate far from the dissociate interface but the carriers recombine before reaching the electrode.

Consequently, the 6T would seem then the best candidate for the realization of organic photovoltaic cells, because on the one hand a weaker gap and on the other hand conductivity and mobility more significant. This tendency is confirmed by the big successes which know the oligothiophene as an active component in the organic photovoltaic cells [18].
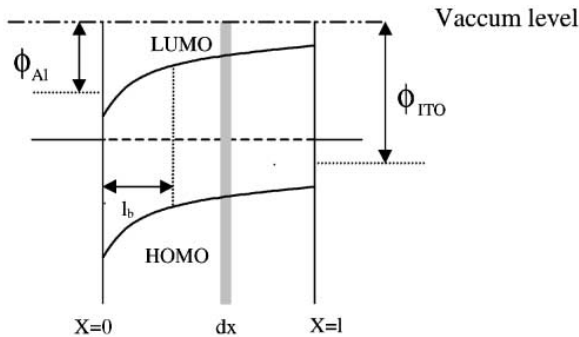

Fig. 8. Energy diagram of ITO/6T/Al structure.

These results can be better understood on the basis of the following model. In fact, Gosh and al. [19] have shown in 1974 that photo-excitation with energy equal or larger than the energy gap of the material generate electron–holes pair in a narrow photoactive region, the depletion layer which leads to free charge carriers in the bulk (**Fig. 8**). They have also shown that the most photosensitive region is the interface between the Al and the active area (6T), and that the photocurrent depends on the ability of the minority carriers (electrons) to reach this interface. The density of photo-produced carriers within dx at a distance x from the Al/6T interface is:

$$dn = \eta_q \, \phi \, \alpha \, e^{-\alpha x} \, dx \qquad (1)$$

where ϕ is the flux density of incident photons (cm² s⁻¹), α the absorption coefficient (cm⁻¹), and η_q the quantum efficiency.

The illumination of the Al side, the carriers' density that reaches the junction is given by:

$$n_{Al} = \eta_q \phi \left(\left(1 - e^{-\alpha l_b}\right) + \frac{\alpha}{(\alpha + B)} \left(e^{\alpha l_b} - e^{-\alpha l} e^{-B(l - l_b)} \right) \right) \qquad (2)$$

where the first term indicates the term of the carriers created in the width barrier l_b and the second term present carriers create in the thickness ($l - l_b$). L is the diffusion length of carriers ($L = \frac{1}{B}$). The photocurrent measured in illuminate on Al is proportional to carrier density.

We confronted our experimental results with the Gosh model (**Fig. 9**) and we noticed whereas the model accounts well for the variation of the photocurrent in weak energies but that the spectrum of action calculated deviates appreciably from the experimental spectrum to strong energies. Then this model does not well justify the experimental results, especially the behavior of the photocurrent for the incidental photons with strong energy. As this fact, we made a modification to this model which to hold account the dissociation of strongly bound exciton photo-induced at the temperature T with a probability proportional to: $\exp\left(\frac{h\nu - E_g}{kT} \right)$, where E_g is the gap of sexithiophene. Then the new expression of photocurrent is in the form:

$$J_{Al} \propto \exp\left(\frac{h\nu - E_g}{kT} \right) \eta_q \phi \left(\left(1 - e^{-\alpha l_b}\right) + \frac{\alpha}{(\alpha + B)} \left(e^{\alpha l_b} - e^{-\alpha l} e^{-B(l - l_b)} \right) \right) \qquad (3)$$
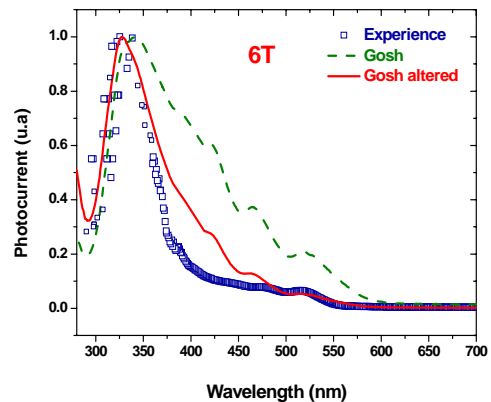

Fig. 9. Action spectrum of cell based on 6T after modeling by Gosh and Gosh altered.

Adjustment of the experimental spectra of the 6T obtained by illumination in side of aluminum, show a better agreement of the model of Gosh altered with the experiment on the totality of the spectral field (Fig.9) We can estimate then the quantum yield $\eta_q = 0.1$ and the flux density $\phi = 10^{15}$ photons/cm². Otherwise, in our case the carriers in 6T are mainly holes, and if we consider the statistical nature of the diffusion, we can consider that the holes reach the active area more easily than the electrons. Thus we can estimate starting from model of Gosh altered (Fig.9) that the electrons diffusion length is $L \approx 10^{-6}$cm, the diffusion holes length is $L_p \approx p/n.L_n \approx 10^{-5}$ cm. Moreover the width of barrier is $l_b \approx 10^{-5}$cm which is about equal to the thickness of film. The carrier mobility is about 2.510^{-6} cm²/Vs. These values are close to cells deferred by other auteurs 0[22] and are located in the same fields as those of the molecular crystals.

3.3 Photovoltaic response of devices with SAM

We investigate in this part the grafting effect of self-assembled monolayer of benzoic acid molecules (ABA and NBA) on ITO in a sexithiophene based photovoltaic cell (Fig. 3), to improve there photovoltaic performance. The current density-voltage characterization under illumination of samples has shown different characteristics depending on the SAM nature (Fig.10a, Fig.10b). The table 3 shows the values of photocurrent (J_{ph}), open circuit voltages (V_{OC}) and the efficiencies of devices with and without SAMs of benzoic acids.

Fig. 10. Characteristics I-V of studied structure under illumination on side of Al with Xenon lamp Linear plot and (b) log(J) vs.log(V) plot

Table 3: Photovoltaic parameters of devices after illumination by Xenon lamp.

	V_{OC} (V)	Jsc (µA/cm²)	FF(%)	$(\eta \pm 0,1) \times 10^{-2}$ (%)
ITO/6T/Al	1,18	0,48	28,75	2,7
ITO/ABA/6T/Al	1,24	1,08	21,73	4,9
ITO/NBA/6T/Al	0,24	0,83	31,97	1,1

This results prove that ITO/ABA/6T/Al cell show largest short–circuit current (J_{sc}) and potential of open circuit (V_{OC}). However for the cell ITO/NBA/6T/Al, we notice a significant reduction of the value of V_{OC} with a weak increase in photocurrent. We can explain this note by a considerable photogeneration of the carriers after functionalization of the anode by ABA. In addition the influence of these dipolar molecules on the efficiency shows a reduction for ITO/NBA/6T/Al by up two orders of magnitude for sample with SAM of ABA and reduction of two orders of magnitude by report to bare ITO, because the low value of maximum power and V_{OC}, but this efficiency are very close to that obtained in the literature [3]. This improvement is attributed to an enhanced interfacial charge collection of photogenerate carriers. Also the orientation of dipole moment of SAM in the direction favor of increase of interfacial energy between the ITO and the SAM. The potential V_{OC} which depend on the interne potentiel (V_{bi}) is a crucial parameter for the optimization of these photovoltaic cells and confirm this explanation. For the purpose, an ideal model was describe
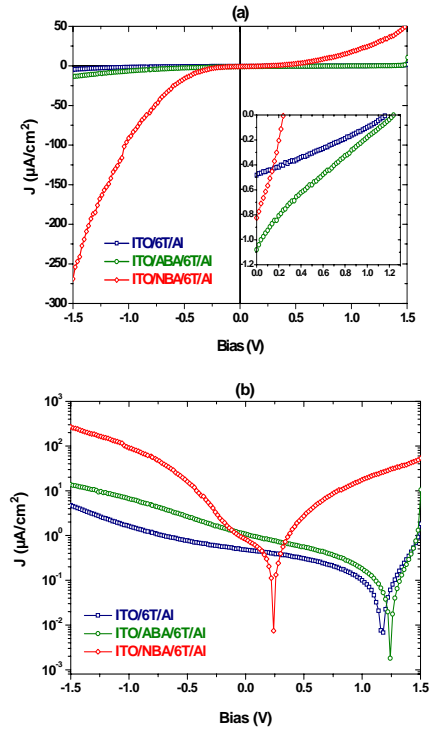
in the literature [23] show that V_{OC} can be affected by the rates of generation of photocarriers to the interfaces with the anode and cathode such envisaged by the following equation:

$$V_{OC} = V_{bi} - \frac{kT}{e} \ln\left(\frac{g_a}{g_c}\right) \qquad (4)$$

where

$$V_{bi} = \left(\phi_{ITO} - \phi_{Al}\right) + \frac{qN\mu_D}{\varepsilon_0.\varepsilon} \qquad (5)$$

g_a and g_c refer to photogenerated holes at the anode and at the cathode. $q = 1.610^{-19}$ C is the majority carrier charge, ε_0 the permittivity of the vacuum and ε is the dielectric constant of molecules SAM ($\varepsilon = 5.3$), µ D dipole moment ($\mu_{NBA} = -5.9D$) and ($\mu_{ABA} = +2.6D$), Γ is the number of molecules by unit surface, that equal to 210^{18} molecules/m² for ABA molecule and 1.310^{18} molecules/m² for NBA molecule [24-25].

From Eq. 4, we can calculate the rate of generation to the anode g_a affected by the SAM layer. We deduce then that increase in ratio g_a/g_c is more significant for NBA (5.17×10^{-4}) that for ABA (2.55×10^{-5}) by comparing with the reference (8.4×10^{-11}). We assume that increase in g_a is more significant than the dipole moment of the layer is large. These results show that the dissociation of excitons in free carriers has done through a gradient of the interne electric potential (V_{bi} greater). Thus NBA compound has a large dipole moment ropes the charge carrier photogeneration of the carriers to the anode, but is oriented in the sight of reduction in photocurrent. On the contrary, ABA where orientated in a direction such as the built-in potential is enhanced, involving creation of excess of the free carriers, and their collection with the electrodes gives a photocurrent that enhanced compared to ITO/6T/Al sample.

4. Conclusion

Study of electrical characteristics of photovoltaic cell base on sexithiophene, show from J-V experimental results that the conduction mechanism dominated by Richardson-Schottky emission in low voltage followed by SCLC theory with an exponential distribution of traps. These results are confirmed by modeling with impedance spectroscopy under various polarizations. The equivalent model includes two circuits RC parallel assembled in series. The absorption and action spectral response indicate that choice of 6T as active layer in our device would seem then the best candidate for conversion photovoltaic, because on the one hand a weaker gap and on the other hand conductivity and mobility more significant. Various parameters e.g. width barrier, diffusion length and mobility of carrier has been determinate by Gosh modeling. We demonstrate from J-V characterization in light, that illumination with Xenon lamp maximizes efficiency of (ITO/6T/Al) structure. Furthermore, grafting of self-assembled dipolar molecules of benzoic acids (ABA and NBA) on ITO substrate improve photovoltaic performance of organic cells. We perceive a significant increase of the efficiency of photovoltaic cell with oriented dipole molecule of ABA at ITO/6T interface of 0.05% reported with NBA. This improvement is affected by efficient dissociation of geminate electron-hole pairs that enhance the charge carrier photogeneration therefore the power-conversion efficiency of organic photovoltaic devices.

References

[1] J. M. Nunzi, C. R. Physique **3**, 523 (2002).
[2] N. S Sariciftci, L. Smilowitz, A. J Heeger, F. Wudl. Science **258**, 1474 (1992).
[3] C. J Brabec, N. S Sariciftci & Hummelen. Adv. Funct. Mater. **11**, 1526 (2001).
[4] S. F. Alvarado, P. F. Seidler, D. G. Lidzey Al. Phys. Rev. Lett., **81**. 1082 (1998).
[5] X. Crispin, Solar Energy Mater. Solar Cells **83**, 147 (2004).
[6] C.W. Tang, Appl. Phys. Lett. **48,** 183 (1986).
[7] C. Videlot, A. El Kassmi, D. Fichou, Solar Energy Materials & Solar Cells **63**, 69 (2000).
[8] T. Otsubo, Y. Aso, K. Takimiya. J. Mater. Chem. **12**, 2565 (2002).
[9] M. Carrara, F. Nüesch, L. Zuppiroli. Synthetic Metals. **121**, 1633 (2001).
[10] R. A. Hatton, M. R. Willis, M. A. Chesters, F. J. M. Rutten, D. Briggs, J. Mater. Chem. **13**, 38 (2003)
[11] Lai-Wan Chong, Yuh-Lang Lee, Ten-Chin We Thin Solid Films. **515**, 2833 (2007)
[12] H. Bedis Ouerghemmi, F. Kouki, P. Lang, H. Ben Ouada, H. Bouchriha. Syn. Metal, **159**, 551 (2009)
[13] J. Nakahara, T. Konishi, S. Murabayashi, M. Hoshino, Heterocycles. **26**, 1793 (1987).
[14] J. Kagan, S. K. Arora, J. Org. Chem. **48**, 4317 (1983).
[15] S. H. Kim, K. H. Choi, H. M. Lee, D. H. Hwang, et al. J. Appl. Ph**y**s. **87**, 882 (2000).
[16] P. Delonnoy, G. Horowitz, H. Bouchriha, J. L. Fave, F. Garnier, at al. Synth. Met. **67**, 197 (1994).
[17] F. Kouki, H. Bedis Ouerghemi & H.Bouchriha: "Effect of the oligothiophene molecules length on the performances of organic photovoltaic cell", submitted.
[18] C. R. McNeill, M. J. Clifton-Smith et al, Current Applied Physics, **4**, 335 (2004)
[19] A. K. Ghosh, D. L. Morel, T. Feng, R. F. Shaw, Journal of Applied Physics, **45**, N°1, (1974).
[20] B. Servet, G. Horowitz, S. Ries, O. Lagorsse, P . Lang, F. Garnier et al, Chemical Mater. **6**, 1809 (1994).
[21] N. Loussaif, L .Hassine, N. Boutabba, F. Kouki et al, Synthetic Metals; **128**, 283 (2002).
[22] L. Si-Ahmed. Doctorat these of polytechnic Federal School-Lausanne, (1999).
[23] G. G. Malliaras, J. C. Scott, Al. Journal of Applied Physics, **84**, N° 3 (1998).
[24] H. Bässler, H. Killesreiter, G. Vaubel, Discuss. Faraday Soc. **51**, 48 (1971).
[25] L. Zuppiroli1, L. Si-Ahmed1, K. Kamaras1, F. F. Nüesch, Al. Eur. Phys. J. B **11**, 505 (1999).

*Corresponding author: hanene.bedis@fst.rnu.tn